

This is the accepted manuscript made available via CHORUS. The article has been published as:

## In situ tunable g factor for a single electron confined inside an InAs quantum dot molecule

W. Liu, S. Sanwlani, R. Hazbun, J. Kolodzey, A. S. Bracker, D. Gammon, and M. F. Doty

Phys. Rev. B **84**, 121304 — Published 16 September 2011

DOI: [10.1103/PhysRevB.84.121304](https://doi.org/10.1103/PhysRevB.84.121304)

# In-situ tunable g factor for a single electron confined in a quantum dot molecule

W. Liu<sup>1</sup>, S. Sanwlani<sup>1</sup>, R. Hazbun<sup>2</sup>, J. Kolodzey<sup>2</sup>, A. S. Bracker<sup>3</sup>, D. Gammon<sup>3</sup>, and M. F. Doty<sup>1\*</sup>

<sup>1</sup>*Department of Materials Science and Engineering, University of Delaware*

<sup>2</sup>*Department of Electrical and Computer Engineering, University of Delaware and*

<sup>3</sup>*Naval Research Laboratory, Washington, D.C.*

Tailoring the properties of single spins confined in self-assembled quantum dots (QDs) is critical to the development of new optoelectronic logic devices. However, the range of heterostructure engineering techniques that can be used to control spin properties is severely limited by the requirements of QD self-assembly. We demonstrate a new strategy for rationally engineering the spin properties of single confined electrons or holes by adjusting the composition of the barrier between a stacked pair of InAs QDs coupled by coherent tunneling to form a quantum dot molecule (QDM). We demonstrate this strategy by designing, fabricating, and characterizing a QDM in which the g factor for a single confined electron can be tuned in situ by over 50% with a minimal change in applied voltage.

PACS numbers: 78.20.Ls, 78.47.-p, 78.55.Cr, 78.67.Hc

## I. INTRODUCTION

The spin projections of a single confined electron or hole provide a natural two-level system that could serve as the logical basis for classical and quantum information processing devices.<sup>1,2</sup> Single spins confined in self-assembled quantum dots (QDs) are especially promising because they have relatively long decoherence times and can be manipulated rapidly by optical pulses.<sup>3-5</sup> Tailoring the properties of these confined single spins is critical to the development of new optoelectronic devices.<sup>6</sup> Although there are many heterostructure engineering techniques that can be used to tune the properties of spin ensembles,<sup>7-9</sup> the range of techniques that can be applied to single QDs, and thus to single confined spins, is severely limited by the requirements of QD self-assembly.

In this Letter we show that previously inaccessible heterostructure engineering techniques can be applied to a single confined spin by adjusting the composition of the barrier between a stacked pair of InAs QDs coupled by coherent tunneling to form a quantum dot molecule (QDM). We demonstrate this strategy by designing, fabricating, and characterizing a QDM in which the g factor for a single confined electron can be tuned in situ by over 50% with a change in applied voltage of less than 70 mV. In situ tuning of the g factor, which determines the Zeeman splitting between spin projections, provides a powerful tool for manipulating spins.<sup>9-11</sup> Applications include tuning individual bits into resonance with magnetic fields, GHz frequency spin manipulation, conversion between photon and solid-state qubits, and suppression of decoherence originating in fluctuating nuclear magnetic fields.<sup>8,12-14</sup>

Several approaches to tuning the excitonic g factor of individual QDs have been reported,<sup>15</sup> including a 250% change in the neutral exciton g factor as a function of the electric field applied to single height-engineered InGaAs/GaAs QDs.<sup>16</sup> However, in<sup>16</sup> the large applied electric field also ejects charge carriers from the QD, rendering this and similar approaches unsuitable for control of

a single confined spin. The largest reported g factor tuning for a single spin confined in a solid-state system is the 400% change in the g factor of a single hole confined in an InGaAs/GaAs QDM,<sup>17-19</sup> which is understood to arise when the controllable formation of delocalized molecular orbitals alters the amplitude of the hole wavefunction in the GaAs barrier between the QDs. Here we demonstrate that the formation of molecular orbitals in QDMs can be rationally engineered to create tailored properties for single confined electrons or holes.

Previous approaches to engineering the g factor of single holes rely on the natural difference in hole g factor between the InGaAs QD and the GaAs barrier.<sup>16,17</sup> Unfortunately, the g factor of an electron in an InGaAs QD (typically about -0.5) is almost the same as in bulk GaAs (-0.44).<sup>17,20</sup> Consequently, these approaches cannot be used to create tunable g factors for single electrons.<sup>17</sup> The new approach described here uses rational engineering of delocalized molecular orbitals in QDMs with systematically engineered barrier composition to create a tailored and in-situ tunable g factor for a single electron. The molecular orbitals have symmetric (anti-symmetric) wavefunctions that have an increased (decreased) amplitude in the barrier. Because the formation of molecular orbitals is a resonant effect, small changes in the electric field applied to the QDM generate large changes in the Zeeman splitting (g-factor). Unequal Zeeman splitting of symmetric and anti-symmetric orbitals is equivalent to spin-dependent tunneling, so this approach can be used to engineer spin properties for a wide variety of device applications.<sup>18</sup> The spins remain confined in the QDM structure and accessible to optical manipulation throughout the tuning range.

## II. QDM DESIGN AND CHARACTERIZATION

Our design for a QDM that has a tunable g factor for a single confined electron introduces 3 nm of  $\text{Al}_x\text{Ga}_{1-x}\text{As}$  into the barrier separating two InGaAs QDs (Fig. 1a).

The  $\text{Al}_x\text{Ga}_{1-x}\text{As}$  is sandwiched between two 3 nm layers of GaAs so that the dynamics of QD self-assembly and capping remain similar to existing QDM growth protocols.  $\text{Al}_x\text{Ga}_{1-x}\text{As}$  has an electron g factor that rises from -0.44 to +2 as the Al fraction (x) increases from 0 to 100%.<sup>21</sup> Although pure AlAs would introduce the largest positive g factor contribution, it would also dramatically reduce the probability of electron tunneling through the barrier, and therefore reduce the amplitude of the molecular wavefunction in the barrier. We choose  $\text{Al}_{0.3}\text{Ga}_{0.7}\text{As}$  to create a positive contribution to the electron g factor while preserving a moderate amplitude for the wavefunction in the barrier.

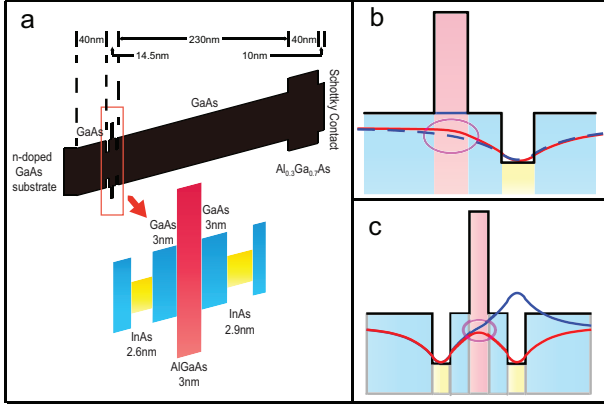


FIG. 1: (Color Online) (a) Band structure of the MBE grown InAs/GaAs/AlGaAs sample. (b) Calculated wavefunction of a single electron confined in a single QD without (dashed) and with (solid) inclusion of the AlGaAs layer. (c) Calculated molecular wavefunctions for a single electron delocalized over the entire QDM.

Fig. 1b shows the calculated wavefunction for a single electron localized in the top QD with (solid line) and without (dashed line) the inclusion of  $\text{Al}_{0.3}\text{Ga}_{0.7}\text{As}$ . Fig. 1c shows the calculated symmetric and antisymmetric wavefunctions for a single electron in a molecular state formed by coherent tunneling between the two QDs. Calculations were performed with a finite element method Schrödinger solver based on an 8 band k.p model and a Lagrangian formulation for systems subject to constraints.<sup>22,23</sup> The probability amplitude of these molecular wavefunctions in the AlGaAs region determines the AlGaAs contribution to the g factor.

We grew the designed QDM by molecular beam epitaxy and characterized the single electron g factor using magneto-optical studies of single QDMs.<sup>22</sup> We present measurements of a single QDM that is representative of the six we have measured. Fig. 2 presents the energy of the photoluminescence (PL) lines emitted by the QDM as a function of applied electric field when no magnetic field is applied. Because the data are acquired with long integration times, random optical charging events permit us to observe several different charge states in a single spectrum.<sup>24,25</sup> The characteristic anticrossings and en-

ergy shifts allow us to unambiguously assign the blue symbols to the neutral exciton ( $X^0$ : one electron and one hole), the red symbols to the biexciton ( $XX^0$ : two electrons and two holes) and the black symbols to the doubly negatively charged exciton ( $X^{2-}$ : three electrons and one hole).<sup>22,24</sup>

### III. MEASURING A TUNABLE G FACTOR FOR A SINGLE ELECTRON SPIN

The  $X^0$  PL (blue symbols) in Fig. 2 originates in a state that has one electron and one hole. The QD size asymmetry and applied electric field cause the hole to remain localized in the top QD, as schematically depicted in the inset.<sup>26</sup> When the electron energy levels of the two QDs are not in resonance the electron is localized in either the top or bottom QD. When the applied electric field tunes the electron levels into resonance, coherent tunneling leads to the formation of the delocalized molecular orbitals and an avoided crossing between the two possible spatial configurations of the electron. The molecular orbital character of the delocalized states is schematically depicted in the insets.

We now show that the excitonic g factor depends on the applied electric field and that the tunability can be attributed to a changing g factor for the single confined electron as a consequence of the formation of these molecular states. We measure the excitonic g factor via the Zeeman splitting of the  $X^0$  PL lines as a function of applied magnetic field. We first measure the Zeeman splitting away from a molecular resonance (e.g. the PL line at 1338 meV and a static electric field of 21.50 kV/cm in Fig. 2) so that the electron levels are not in resonance and the electron and hole are confined in the top QD. The calculated electron wavefunction presented in Fig. 1b demonstrates that inclusion of the AlGaAs alters the wavefunction distribution for a single electron confined in the top QD, and therefore likely alters the single electron g factor. The effect of the AlGaAs on holes is expected to be significantly weaker because the large effective mass for the hole results in a wavefunction more tightly confined to the QD. The experimental results<sup>22</sup> indicate that the excitonic g factor for the top QD is 1.45, but the independent contributions of the electron and hole cannot be determined from this measurement.

To show that the electron g factor can be tuned by the formation of molecular states, we track the Zeeman splitting as a function of applied electric field through the  $X^0$  anticrossing at  $F_{x^0}$ , indicated in Fig. 2 by the right red box. The symbols in Fig. 3a plot the energy splitting between the two molecular orbital branches of the electron anticrossing. The minimum of the energy splitting provides a direct measurement of the strength of the tunnel coupling. The hyperbolic fit to this data reveals that the electron energy levels are in resonance at  $F_{x^0} = 17.48 \text{ kV/cm}$  and that the tunneling matrix element ( $t_{x^0}$ ) is 0.75 meV. This measured value of  $t_{x^0}$  agrees

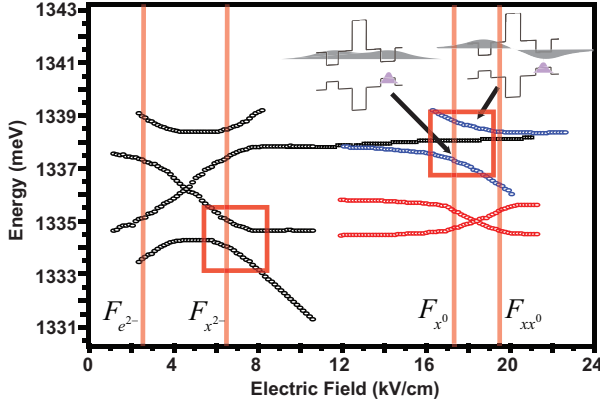


FIG. 2: (Color Online) Measured energy of PL lines emitted from the neutral exciton ( $X^0$ , blue), biexciton ( $XX^0$ , red) and doubly charged negative trion ( $X^{2-}$ , black) states. Purple symbols in the inset schematically indicate the hole wavefunction localized in the top dot. Grey symbols schematically indicate the orbital character of the molecular electron states formed by coherent tunneling.

well with the calculated tunneling matrix element for the molecular states shown in Fig. 1c (0.79 meV).

In Fig. 3b we plot the Zeeman splitting of each molecular orbital state as a function of applied electric field when a static 8T magnetic field is applied in the Faraday geometry. The Zeeman splitting is directly proportional to the g factor, Bohr magneton, and applied magnetic field, but only the g factor can vary with applied electric field. We plot the splitting in units of the absolute value of the excitonic g factor. A clear resonant change is evident. Electrons in a symmetric molecular orbital (black points) have large wavefunction amplitude in the AlGaAs barrier, so the positive contribution from the AlGaAs offsets the negative contribution from the InGaAs QDs. As a result, the Zeeman splitting of the symmetric orbital is suppressed on resonance. In contrast, the splitting of the antisymmetric orbital (red points) is enhanced because the node of the antisymmetric wavefunction suppresses the electron wavefunction in the AlGaAs and makes the g factor more negative. The absolute value of the excitonic g factor can be tuned by 50%, from 1.15 to 1.76, with small changes in the applied electric field.

We fit the resonant changes in g factor using<sup>17</sup>:

$$g_T^B(F) = g_T \pm \frac{2t_{X^0}g_{12}}{\sqrt{e^2d^2(F - F_e)^2 + 4t_{X^0}^2}}$$

where  $g_T = g_e + g_h$  is the g factor for the exciton recombination, including Zeeman splitting from the electron and hole in the initial state.  $g_e$  is the g factor for a single electron confined in either QD at applied electric fields for which tunnel coupling is negligible. The g factors for single electrons in both QDs are taken to be identical because PL lines that have electrons in different QDs asymptote to the same Zeeman splitting away

from the anticrossing resonance.  $g_h$  is the g factor for the single hole and does not depend on the applied electric field because the hole remains localized in the top QD.  $e$  is the electron charge,  $d$  is the separation between the QDs and  $F$  is the applied electric field.  $F_{x^0}$  and  $t_{x^0}$  are obtained from Fig. 3a. The measured resonant change in g factor (Fig. 3b) peaks at exactly  $F_{x^0}$ . The measured width of the resonance shows excellent agreement with the g factor model, in which the resonance width is determined only by the independently measured value of  $t_{x^0}$ . The agreement with the model confirms that the resonant change in g factor comes from the formation of delocalized molecular states for a single electron.

The only free parameter in the fit is  $g_{12}$ , which represents the contribution from the barrier and determines the amplitude of the resonant change in Zeeman splitting. We find best agreement with the data for  $g_{12} = 0.33$ . This positive value of  $g_{12}$  validates our design strategy.<sup>21</sup> Additional validation of our model comes from the measured resonant change in g factor due to the tunneling of a single electron in the doubly negatively charged exciton state ( $X^{2-}$ ).<sup>25</sup> The black symbols in Fig. 2 indicate the energy of PL emitted by the  $X^{2-}$  state. Anticrossings occur in both the initial state and the two-electron ( $e^{2-}$ ) final state, resulting in the characteristic “X” shape.<sup>21</sup> The anticrossings occur at slightly different electric fields because of Coulomb and exchange interactions.<sup>25,27</sup> Calculated energy level diagrams for the initial states, final states and the excitonic PL verify that the anticrossing at  $F_{x^{2-}}$  arises from tunneling of a single electron in the presence of an additional two electrons and one hole.<sup>22</sup>

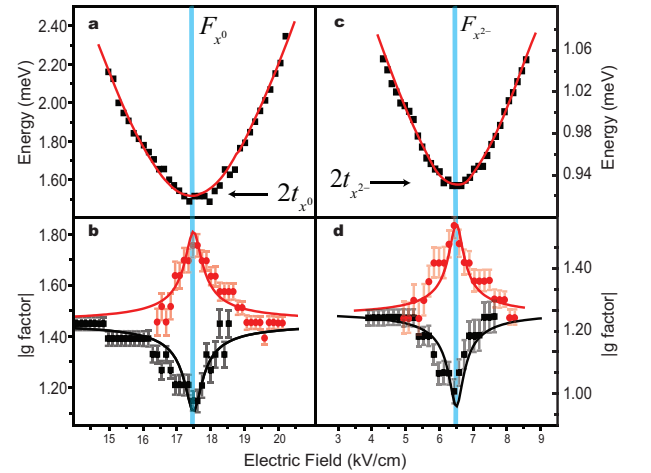


FIG. 3: (Color Online) (a) Energy difference between the two anticrossing branches of the neutral exciton ( $X^0$ ). The red line is a hyperbolic fit to the data. (b) Zeeman splitting of the bonding and antibonding states as a function of electric field (symbols) for the neutral exciton. Solid line is a fit as described in the text. (c,d) As in (a,b) for the two orbital states of the doubly negatively charged exciton ( $X^{2-}$ ). The data for b and d are taken at 8 Tesla.

The symbols in Fig. 3c plot the energy separation between molecular orbital branches of the  $X^{2-}$  anticrossing. The hyperbolic fit to the data indicates that  $F_{x^{2-}} = 6.50 \text{ kV/cm}$  and  $t_{x^{2-}} = 0.47 \text{ meV}$ . Fig. 3d presents the resonant change in g factor from the Zeeman splitting of the  $X^{2-}$  molecular orbital branches. The resonant change in g factor peaks at  $F_{x^{2-}}$  and agrees with our model fit using  $t_{x^{2-}}$ . The slight shifts in asymptotic g factor, tunneling strength, and resonant contribution from the barrier, relative to the neutral exciton case, indicate that Coulomb interactions may perturb the wavefunction amplitudes. These Coulomb interactions could provide an additional tool for controlling spin interactions, but require further exploration. The observation of a resonant change in g factor at the  $X^{2-}$  anticrossing confirms that the tunable g factor arises from the formation of molecular orbitals for a single tunneling electron.

Although we are unable to independently measure the hole and electron g factors for the QDM presented here, measurements of other QDMs in this and similar samples reveal that the hole g factor is typically between 1.1 and 1.7. Consequently, the design presented here prob-

ably tunes the electron g factor very close to zero. For example, if we take a hole g factor of 1.2 we find that the electron g factor in this QDM is tuned from 0.56 to -0.05 in the  $X^0$  case and from 0.3 to -0.2 in the  $X^{2-}$  case.

We have demonstrated that inclusion of an  $\text{Al}_{0.3}\text{Ga}_{0.7}\text{As}$  layer in the barrier region of a QDM allows us to tune the excitonic g factor by 50% using a small change in applied bias. The experimental results and analysis confirm that this tuning is due to the formation of delocalized molecular states that change the g factor for a single confined electron. This result therefore provides a clear demonstration of a new strategy for rationally engineering the spin properties of single confined electrons or holes.

### Acknowledgments

This research is financially supported by the University of Delaware Research Foundation, NSA and NSF award #0844747.

---

\* Electronic address: [doty@udel.edu](mailto:doty@udel.edu)

- <sup>1</sup> F. H. L. Koppens, J. A. Folk, J. M. Elzerman, R. Hanson, L. H. W. van Beveren, I. T. Vink, H. P. Tranitz, W. Wegscheider, L. P. Kouwenhoven, and L. M. K. Vandersypen, *Science* **309**, 1346 (2005).
- <sup>2</sup> D. Loss and D. P. DiVincenzo, *Physical Review A* **57**, 120 (1998).
- <sup>3</sup> D. Brunner, B. D. Gerardot, P. A. Dalgarno, G. Wust, K. Karrai, N. G. Stoltz, P. M. Petroff, and R. J. Warburton, *Science* **325**, 70 (2009).
- <sup>4</sup> E. D. Kim, K. Truex, X. D. Xu, B. Sun, D. G. Steel, A. S. Bracker, D. Gammon, and L. J. Sham, *Physical Review Letters* **104**, 4 (2010).
- <sup>5</sup> D. Kim, S. Carter, A. Greulich, A. Bracker, and D. Gammon, *Nature Physics* (2010).
- <sup>6</sup> A. Shields, *Nature Photonics* **1**, 215 (2007).
- <sup>7</sup> G. Salis, Y. Kato, K. Ensslin, D. C. Driscoll, A. C. Gossard, and D. D. Awschalom, *Nature* **414**, 619 (2001).
- <sup>8</sup> Y. Kato, R. Myers, D. Driscoll, A. Gossard, J. Levy, and D. Awschalom, *Science* **299**, 1201 (2003).
- <sup>9</sup> M. Poggio, G. M. Steeves, R. C. Myers, N. P. Stern, A. C. Gossard, and D. D. Awschalom, *Physical Review B* **70**, 121305(R) (2004).
- <sup>10</sup> W. Sheng, *Applied Physics Letters* **95**, 113103 (2009).
- <sup>11</sup> C. E. Pryor and M. E. Flatte, *Applied Physics Letters* **88**, 233108 (2006).
- <sup>12</sup> M. Atatüre, J. Dreiser, A. Badolato, A. Hoge, K. Karrai, and A. Imamoglu, *Science* **312**, 551 (2006).
- <sup>13</sup> E. Yablonovitch, H. Jiang, H. Kosaka, H. Robinson, D. Rao, and T. Szkopek, *Proceedings of the IEEE* **91**, 761 (2003).
- <sup>14</sup> A. V. Khaetskii, D. Loss, and L. Glazman, *Physical Review Letters* **88**, 186802 (2002).
- <sup>15</sup> D. Kim, W. Sheng, P. Poole, D. Dalacu, J. Lefebvre, J. La-

- pointe, M. Reimer, G. Aers, and R. Williams, *Physical Review B* **79**, 045310 (2009).
- <sup>16</sup> F. Klotz, V. Jovanov, J. Kierig, E. C. Clark, D. Rudolph, D. Heiss, M. Bichler, G. Abstreiter, M. S. Brandt, and J. J. Finley, *Applied Physics Letters* **96**, 53113 (2010).
- <sup>17</sup> M. F. Doty, M. Scheibner, I. V. Ponomarev, E. A. Stinaff, A. S. Bracker, V. L. Korenev, T. L. Reinecke, and D. Gammon, *Physical Review Letters* **97**, 197202 (2006).
- <sup>18</sup> M. F. Doty, J. I. Climente, M. Korkusinski, M. Scheibner, A. S. Bracker, P. Hawrylak, and D. Gammon, *Physical Review Letters* **102**, 47401 (2009).
- <sup>19</sup> T. Andlauer and P. Vogl, *Physical Review B* **79**, 45307 (2009).
- <sup>20</sup> M. Bayer, O. Stern, A. Kuther, and A. Forchel, *Physical Review B* **61**, 7273 (2000).
- <sup>21</sup> H. Kosaka, A. A. Kiselev, F. A. Baron, K. W. Kim, and E. Yablonovitch, *Electronics Letters* **37**, 464 (2001).
- <sup>22</sup> see EPAPS document.
- <sup>23</sup> L. R. Ram-mohan, *Finite Element and Boundary Element Applications to Quantum Mechanics* (Oxford University Press, New York, 2002).
- <sup>24</sup> E. A. Stinaff, M. Scheibner, A. S. Bracker, I. V. Ponomarev, V. L. Korenev, M. E. Ware, M. F. Doty, T. L. Reinecke, and D. Gammon, *Science* **311**, 636 (2006).
- <sup>25</sup> M. Scheibner, M. Doty, I. Ponomarev, A. Bracker, E. Stinaff, V. Korenev, T. Reinecke, and D. Gammon, *Phys. Rev. B* **75** (2007).
- <sup>26</sup> A. S. Bracker, M. Scheibner, M. F. Doty, E. A. Stinaff, I. V. Ponomarev, J. C. Kim, L. J. Whitman, T. L. Reinecke, and D. Gammon, *Applied Physics Letters* **89**, 233110 (2006).
- <sup>27</sup> M. F. Doty, M. Scheibner, A. S. Bracker, and D. Gammon, *Physical Review B* **78**, 115316 (2008).